Available online at www.sciencedirect.com

SciVerse ScienceDirect

Ceramics International 39 (2013) 2331–2341

CERAMICS INTERNATIONAL

www.elsevier.com/locate/ceramint

Dielectric, magnetoelectric and magnetodielectric properties in CMFO-SBN composites

S.R. Jigajeni[a], A.N. Tarale[b], D.J. Salunkhe[b], P.B. Joshi[b,*], S.B. Kulkarni[c]

[a]*Walchand Institute of Technology, Solapur, India*
[b]*School of Physical Sciences, Solapur University, Solapur 413255, India*
[c]*Department of Physics, Institute of Science, Mumbai, India*

Received 18 June 2012; received in revised form 13 August 2012; accepted 28 August 2012
Available online 5 September 2012

Abstract

The paper reports synthesis of $Sr_{0.5}Ba_{0.5}Nb_2O_6$ (SBN) and $Co_{1.2-x}Mn_xFe_{1.8}O_4$ (CMFO) via ceramic and hydroxide co-precipitation routes respectively. The nanopowders of SBN-CMFO0.1 (MSBN0.1) and SBN-CMFO0.3 (MSBN0.3) are compacted to form the desired magnetoelectric (ME)/magnetodielectric (MD) composites. The Bi_2O_3 is used as a sintering aid. The Bi_2O_3 at three weight percent is observed to cause agglomeration of SBN and CMFO particles and improve the magneto-mechanical coupling. The composites are investigated for their ferroelectric, ferromagnetic, dielectric, magnetoelectric (ME) and magnetodielectric (MD) properties. The results on the magnetocapacitance (M_c) are observed interesting and could be correctly understood in terms of the stress induced variation in the dielectric constant. The MC is observed to remain fairly constant between 10 to 500 kHz and possess a useful magnitude of M_c nearly 4%.

Keywords: Dielectrics; ME composites; Magnetocapacitance

1. Introduction

The composites of ferroelectric and magnetostrictive compounds are known to exhibit a useful magnitude of magnetoelectric coupling [1–4]. The magnetoelectric effect in these composites is known to be due to stress induced change in remnant polarization of the ferroelectric system in the magnetoelectric composites. Therefore these composites need presence of ferroelectric/relaxor composition possessing a useful value of maximum polarization (P_{max}), remnant polarization (P_r) and piezoelectric coefficient(d), while the magnetostrictive phase is required to possess a large value of resistivity (ρ), magnetostriction (λ) and low value of magnetocrystalline anisotropy energy that is low value of coercive field (H_c). As shall be seen in the next paragraph the $Sr_{0.5}Ba_{0.5}Nb_2O_6$ (SBN) and Mn substituted cobalt ferrite form a correct choice for formation of such compositions [5,6]. Further, recently the laminated ME composites of PZT-$(MnZn)Fe_2O_4$ (MZF) are observed to exhibit useful magnitude of magnetodielectric coupling in the vicinity of electromechanical resonance frequency [7]. This phenomenon was also attributed to the stress induced change in polarization and therefore the dielectric constant. At present the magnetoelectric (ME) effect in such composites is better known but the magnetodielectric (MD) effect has rarely been investigated. Both the ME and MD effects in these systems are possible to be understood in terms of Landau thermodynamic theory as discussed by Zhong and Qiang [8].

Most studies in the past focused on $CoFe_2O_4$, which was applied as one of the constituent of ME composites for its large magnetostriction [9,10]. However the ME voltage coefficient was far smaller than the predicted value due to the poor ME coupling between the $CoFe_2O_4$ and ferroelectric phase probably due to the large anisotropy energy of the $CoFe_2O_4$. Here, substitution of Mn at A or B site is observed to reduce the anisotropy energy and improve the magneto mechanical coupling of the $CoFe_2O_4$. Therefore considering

*Corresponding author. Tel.: +91 9423066675; fax: +91 217 2744768, +91 217 2351300.
E-mail address: drpbjoshi@rediffmail.com (P.B. Joshi).

0272-8842/$ - see front matter © 2012 Elsevier Ltd and Techna Group S.r.l. All rights reserved.
http://dx.doi.org/10.1016/j.ceramint.2012.08.081

virtues of Co and Mn ions in the ferrite system $Co_{1.2-x}Mn_x Fe_{1.8}O_4$ (CMFO) system has been selected as a piezomagnetic phase to form the ME/MD composites [11–14]. As the physical properties of ferrites are dependent on the details of process of synthesis, initially the ferrite system CMFO is synthesized and investigated for its physical and magnetic properties viz. electrical resistivity (ρ), saturation magnetization (M_s), permeability (μ), coercive field (H_c) and coefficient of magnetostriction (λ) as a function of x varying between 0 and 0.4. For the present studies two ferrite compositions are selected to form ME composites, first $x=0.1$ where λ is maximum but ρ is comparatively low and second $x=0.3$ where λ is comparatively low but ρ is high.

Further, the relaxors ferroelectrics are known to have very large electrostrictive response in addition to the piezoelectric coupling, however most relaxors contain Pb, and their lack of remnant polarization makes them unsuitable for piezoelectric applications. An exception is the (Sr, Ba) Nb_2O_6 family which can sustain remnant polarization after polling. Therefore investigations on ME and MD composites with $Sr_{0.5}Ba_{0.5}Nb_2O_6$ (SBN) as a piezoelectric phase are observed interesting [5,6].

Owing to the discussion above the present paper reports synthesis and characterization of two ME and MD composites yMSBN0.1 and yMSBN0.3. In case of yMSBN0.1 $Co_{1.1}Mn_{0.1}Fe_{1.8}O_4$ (CMFO0.1) forms the magnetostrictive phase while for yMSBN0.3 $Co_{0.9}Mn_{0.3}Fe_{1.8}O_4$ (CMFO0.3) is the magnetostrictive phase. Details of formation of composites are discussed further in text. The parent composition CMFO and SBN are initially studied to confirm formation of the required SBN and CMFO phases and crystallite size to be in nanometer range. The paper reports investigations on crystal structure, morphology, dielectric properties, linear magnetoelectric coefficients (α), quadratic magnetoelectric coefficient (β) and the magnetocapacitance (MC), defined through the relation $MC=((\varepsilon(H)-\varepsilon(0))/\varepsilon(0))*100\%$, where $\varepsilon(H)$ and $\varepsilon(0)$ are dielectric constants in presence and absence of magnetic field.

2. Experimental

2.1. Synthesis of CMFO

To achieve near atomic level uniformity of the constituents, the hydroxide co-precipitation route has been adopted for synthesis of $Co_{1.2-x}Mn_xFe_{1.8}O_4$ (CMFO). The Co $(No_3)_2\cdot 6H_2O$, Fe $(NO_3)_3\cdot 9H_2O$ and $MnCl_2$, of AR grade are used as precursors for the hydroxide co-precipitation. The precursors are dissolved in distilled water to form nearly 40 mM solutions of the constituents and NH_4OH is used as precipitant. The precipitates are thoroughly washed in distilled water keeping alkaline medium using NH_4OH (pH-9) [15]. The dried precipitates are calcinated at 1000 °C for 12 h, and final sintering is carried out at 1200 °C for 24 h in two steps with intermediate grinding. The product of final sintering is formed as a powder and also pellets of 1.2 cm diameter. The powder has been used for the formation of magnetoelectric composites, while the pellets are used for determination of ρ, M_s, H_c and λ. To form a magnetoelectric composite the requirement is a high value of ρ, M_s, μ, λ and a low value of H_c.

As discussed earlier the CMFO is initially characterized for determination of these parameters, and Table 1 shows variation of ρ, M_s, H_c, μ and λ as a function of x. The variations of physical parameters are consistent with the values reported earlier for the CMFO system [13]. It could be seen that for $x=$ 0.1 and 0.3, the parameters are optimum for its use as a magnetostrictive phase. For $x=0.1$, λ is maximum but ρ is low and for $x=0.3$, λ is comparatively low but ρ is high. And therefore the CMFO with $x=0.1$ and 0.3 are selected as the magnetostrictive phases.

2.2. Synthesis of SBN

The SBN has been synthesized using standard ceramic route of synthesis because the precursors required for co-precipitation of niobium are not cost effective. Here high purity ($>99.9\%$) $BaCO_3$, $SrCO_3$ and Nb_2O_5 are used as precursors. Considering the earlier reports the calcination and final sintering processes are carried out at 1100 °C for 24 h, and 1250 °C for 12 h, respectively, to form the fine grained SBN powder [16–20]. Due to the calcination and final sintering at 1100 °C and 1250 °C respectively, it is observed that the SBN with the required Tetragonal Tungsten Bronze (TTB) crystal structure and the required relaxor type of behavior, with a diffused phase transition (DPT) in the vicinity of 103 °C, is formed in the present case. These features are discussed in the fourth coming discussion of the paper.

2.3. Formation of composites

The resulting powders of CMFO and SBN are ground thoroughly to form uniform and submicron level particle size. The powders of CMFO and SBN thus formed are used to form the required ME/MD composites using the following formula:

$$(y)\mathrm{CMFO0.1}+(1-y)\mathrm{SBN}+3\%\mathrm{Bi_2O_3w/w} = (y)\mathrm{MSBN0.1} \quad (1)$$

Table 1
Shows the variation of resistivity (ρ), saturation magnetization (M_s), permeability (μ), coercive field (H_c) and coefficient of magnetostriction (λ) for CMFO.

$Co_{1.2-x}Mn_xFe_{1.8}O_4$ x	Resistivity ρ	M_s	H_c(Oe)	μ	λ
0.0	17.96×10^6	265	60	553.62	92
0.1	6.9×10^3	252	68	1154	147
0.2	6.16×10^5	181	67.50	856.15	128
0.3	3.46×10^6	179	52.50	734.0	115
0.4	1.95×10^6	172	60	913.24	65

$$(y)\mathrm{CMFO}0.3+(1-y)\mathrm{SBN}+3\%\mathrm{Bi_2O_3w/w} = (y)\mathrm{MSBN}0.3 \quad (2)$$

where 0.1 and 0.3 represent the content of Mn in CMFO and y is varied from 0.1 to 0.6.

The composites above are termed as yMSBN0.1 and 0.3 respectively during the course of further discussions. Considering the earlier reports, the composites are formed as pellet shaped samples of 1.2 cm diameter and with sintering temperature T_s equal to 1160 and 1225 °C. Three wt percent of Bi_2O_3 is added as a sintering aid to facilitate formation of large grained composites at fairly low sintering temperature. This process may improve the possible magnetomechanical coupling of ME composites [21].

The HP4284A LCR-Q meter is used for the measurements of dielectric constant and complex impedance spectra. Custom built setups are used for the measurements of the resistivity (ρ) and linear and quadratic magnetoelectric coefficient α and β at 850 Hz [22]. To understand the crystal structure of the CMFO, SBN and MSBN composites, Bruker D8 advance XRD spectrometer has been used, while the SEM pictures are obtained using JEOL-JSM 6360 SEM. Further the P–E hysteresis loops are determined using 609B Radian Technologies, USA. Hysteresis loops are measured by making use of high field hysteresis loop tracer designed by Tata Institute of Fundamental Research, Mumbai.

3. Results and discussion

The individual powders of the ferrite and the ferroelectric materials are investigated for structural studies for confirmation of formation of the desired phase and estimation of the crystallite size. The XRD spectrum of CMFO is shown in Fig. 1. The reflections are in confirmation with the JCPD data on cobalt ferrite possessing cubic spinel crystal structure, with lattice parameter 'a' equal to 8.20 Å, which is in confirmation with the earlier reports [13,14]. Further the XRD spectra showed that no peak corresponding to any impurity phase occurs, thus it could be concluded that the CMFO powder of required spinel crystal structure is formed in the present case. Using the Scherrer's formula the crystallite size of CMFO powder is estimated to be 102 nm.

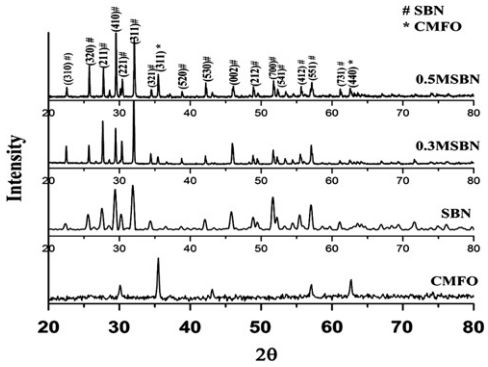

Fig. 1. XRD Spectra for CMFO, SBN and MSBN composites.

Fig. 1 shows the XRD spectrum of SBN powder which shows the reflections corresponding to TTB crystal structure and the spectrum is in confirmation with the earlier reports. The particle size of SBN is observed to be 72 nm as determined using Scherrer formula. The parameters 'a' and 'c' determined from the XRD spectra are $a=b=5.97$ Å and $c=2.46$ Å respectively [23].

Fig. 1 also shows the XRD spectra for composites 0.3MSBN and 0.5MSBN, sintered at 1160 °C for yMSBN0.1. The peaks corresponding to SBN and CMFO are separately identified in the XRD spectra of composites. The XRD spectra for remaining composites are similar with the XRD spectra as shown in Fig. 1.To determine the correlation between variation of relative intensity of the individual phases of CMFO and SBN, the ratio of relative intensities of highest intensity peaks of CMFO and SBN is determined as a function of y. Here Table 2 shows variation of ratio of relative intensities of I_{CMFO}/I_{SBN} corresponding to (311) reflection of CMFO and SBN respectively. From the table it is observed that the relative intensity of (311) reflections of the ferrite phase increases monotonically with increasing y. This feature could be correlated to increasing content of CMFO with y. Thus above observation indicates that pure biphase composites are formed in this process.

3.1. Dielectric, ferroelectric and ferromagnetic properties

Before the discussion of variation of dielectric properties with temperature and frequency, it is required to give consideration to the electrode material and the probable contribution of the electrode in the dielectric properties especially in the low frequency region that is in the vicinity or below 1 kHz [24]. It is observed that the electrode effects are minimum for fired or evaporated silver electrodes on the dielectric materials or composites. Further it is also observed that contribution of the electrode occurs because of the binder material used to form the electrode for example, epoxy resin based silver paste electrode or low melting glass binders in Ag paste etc. [25,26]. Therefore it is advisable to use evaporated silver film or silver paint. In case of silver paint the binding material is evaporated at low temperatures and it is expected that similar to fired or

Table 2
Variation of relative intensities of (311) planes of CMFO and SBN sintered at 1160 °C, yMBSN0.3.

y	I_{CMFO}/I_{SBN}
0.2	0.15
0.3	0.23
0.4	0.44
0.5	0.51
0.6	0.72

evaporated silver, silver paint coated surfaces may provide an alternative electrode possessing very low electrode contribution. Further it is observed that it is possible to model the electrode contribution by making use of impedance spectroscopy [27–29]. Further an important report on the variation of surface potential of polycrystalline $BiFeO_3$ ceramics is also taken into consideration while analyzing the impedance spectra of the composites [30]. Considering these observations the silver paint is employed as an electrode in the present case and using the impedance spectroscopy it is shown that the electrode contribution is fairly small.

Fig. 2 shows variation of dielectric constant (ε) as a function of temperature at 1 kHz for yMSBN0.3 composites sintered at 1160 °C. Here Table 3 shows the values of dielectric constant and electrical quality factor Q at room temperature and at 103 °C. For the purpose of reference the variation of ε for $y=0$ is also shown in Fig. 2. From the figure it is observed that all the compositions exhibit a diffused phase transition (DPT) in the vicinity of 103 °C, consistent with the earlier reports [16–18]. Another interesting observation of ε versus temperature behavior is that the ε increases with temperature in paraelectric region above DPT. This feature is known to occur because of interfacial polarization, occurring at boundaries between the SBN and CMFO phases due to difference in the resistivity of these two phases. Interfacial polarization is known to be predominant at low frequencies and increases as temperature increases [23].

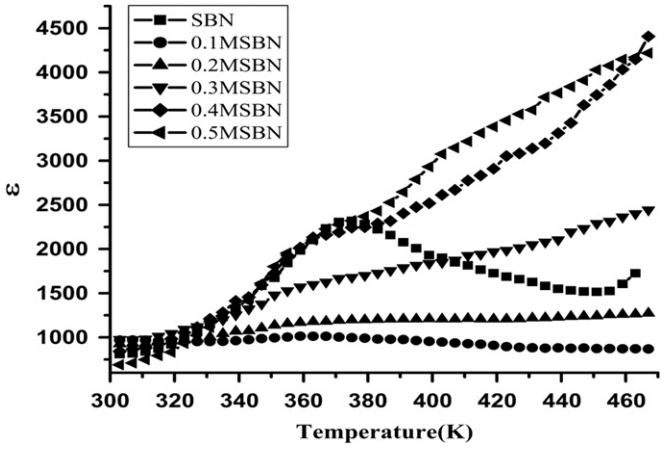

Fig. 2. Variation of ε with temperature at $f=1$ kHz for yMSBN0.3 composites, $T_s=1160$ °C.

Table 3
Variation of dielectric constant ε and Q at 1 kHz for the composites yMBSN0.3 sintered at 1160 °C.

y	ε At Room Temperature	Q At Room Temperature	ε At 103 °C	Q At 103 °C
0.2	925.43	7.68	1198.2	5.86
0.3	975.77	4.28	1701.7	3.68
0.4	841.7	3.22	2246.9	1.87
0.5	689.69	2.57	2368.2	1.28
0.6	565.33	1.89	2725.3	0.83

To investigate this feature further, ε versus T behavior is determined as a function of f for all the compositions. Figs. 3 and 4 show variation of dielectric constant as a function of frequency for 0.4MSBN0.3 and 0.5MSBN0.3 composites sintered at 1160 °C. The behavior for other values of y is similar with behavior as in Figs. 3 and 4. The frequency is varied between 1 kHz and 1 MHz and figures show a diffused phase transition (DPT) in the vicinity of 103 °C corresponding to the SBN phase [16–18]. In this case also, as reported earlier, after the DPT the ε increases with temperature in the paraelectric region above T_c, where the increase in ε with temperature is faster for lower frequencies as compared to the higher ones. Therefore it could be seen that the dielectric constant of the composite consists of two contributions one due to the ferroelectric contribution of SBN and other due to the presence of interfacial polarization at the boundaries between SBN and CMFO phases [5,6,23].

Further from the basic theory of dielectrics and Table 3 it is observed that the magnitude of dielectric constant and electrical quality factor Q are interdependent for a given y. Nevertheless from the table it could be seen that the dielectric constant shows an increasing trend as y increases. With increase in the value of y, the content of SBN decreases in the composition, still it is observed that the dielectric constant increases with increase in y. As discussed earlier, the dielectric constant of the magnetoelectric composites possess two different contributions, one due to the bulk ferroelectric phase and other due to the polarization at the interfaces between ferroelectric and ferromagnetic phases. The present data suggests that the contribution of the interfacial polarization is substantially more than the contribution due to the bulk SBN phase.

To understand the effect of interfacial polarization, the real part ε' and imaginary part ε'' of the complex dielectric constant is also determined. Variation of ε' and ε'' as a

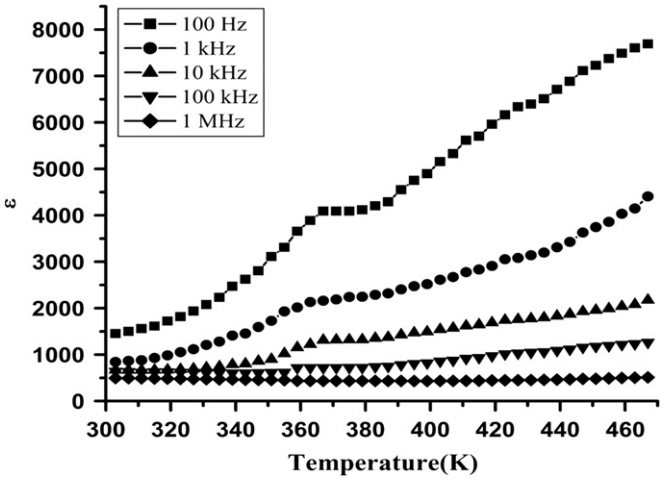

Fig. 3. Variation of ε with temperature of 0.4MSBN0.3 composite, $T_s=1160$ °C.

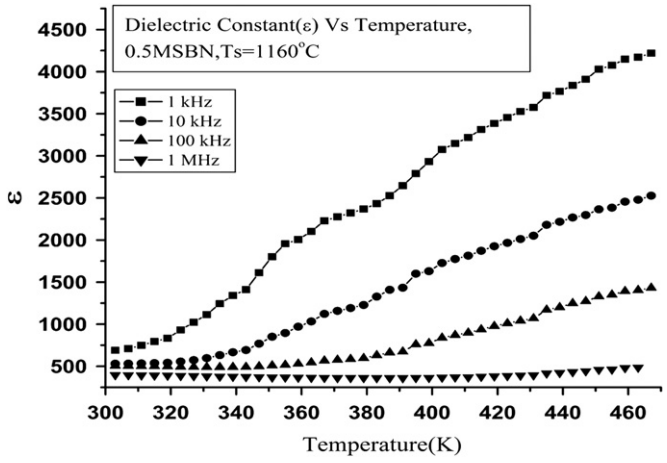

Fig. 4. Variation of ε with temperature of 0.5MSBN0.3 composite, T_s=1160 °C.

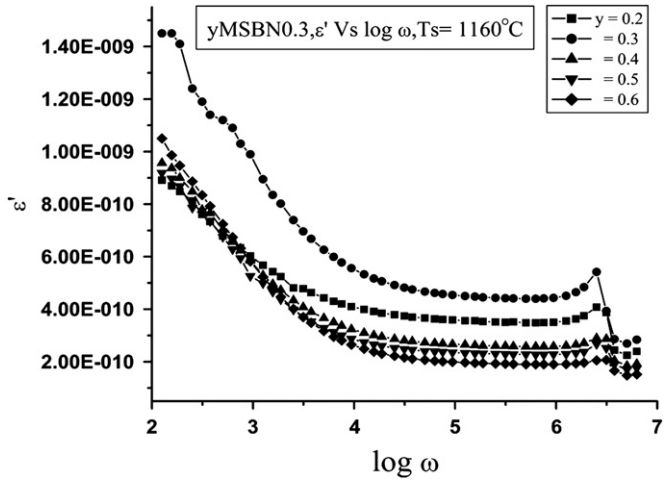

Fig. 5. Variation of ε' with temperature of yMSBN0.3 composite, T_s=1160 °C.

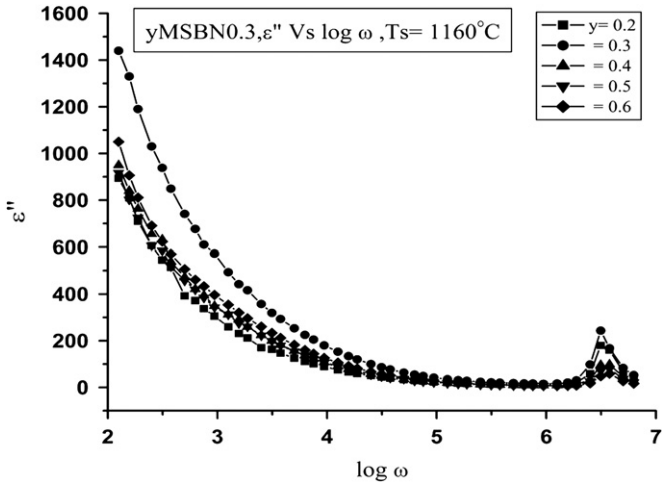

Fig. 6. Variation of ε'' with temperature of yMSBN0.3 composite, T_s=1160 °C.

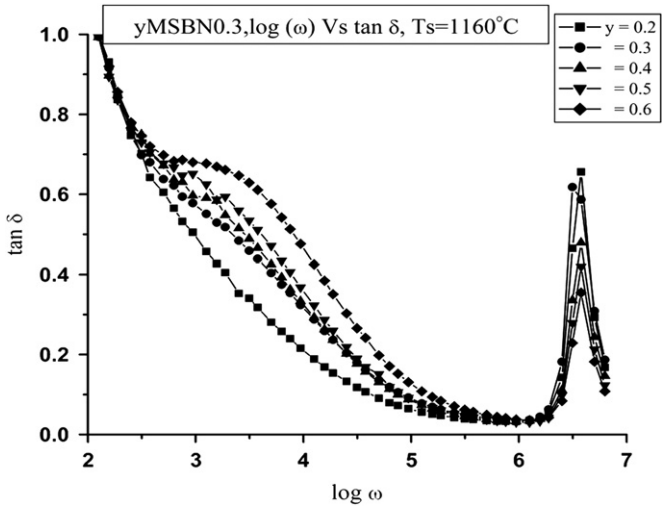

Fig. 7. Variation of tan δ vs. log ω for yMSBN0.3 composites sintered at 1160 °C.

function of frequency are shown in Figs. 5 and 6 for yMSBN0.3 composites sintered at 1160 °C respectively. It is observed that ε' and ε'' decrease rapidly with a very high value at low frequencies and remain constant for higher frequencies. All the samples reveal dispersion due to Maxwell–Wagner type interfacial polarization in agreement with Koops' phenomenological theory [31,32]. The high value of dielectric constant observed at lower frequencies could be explained on the basis of space charge polarization due to inhomogeneous dielectric structure and resistivity of the samples.

It is interesting to record the variation of the loss tangent tan δ as a function of frequency. Fig. 7 shows the variation of tan δ vs. log ω for yMSBN0.3 composites sintered at 1160 °C. It is observed that the variation of tan δ as a function log ω passes through a resonance peak for frequency log ω nearly equal to 6.49 rad/sec^{-1}. Further the loss tangent of all the compositions investigated pass through a resonance peak almost at the same frequency. Additionally the samples in the present case are disc shaped with diameter 1.2 cm. In this situation the tan δ may pass through a resonance where the frequency of ac excitation becomes equal to natural frequency of oscillations of the radial mode. This phenomenon is the electromechanical resonance. Another interesting feature is the occurrence of a resonance peak especially for y=0.4, 0.5 and 0.6 at frequencies nearly equal to 5 kHz. This feature could be attributed to a resonance between dielectric relaxation and frequency of electrical conduction [33]. Here the resonance occurs in tan δ vs. log ω behavior where $1/\tau$, where τ is the relaxation time and is equal to f_0 that is frequency of ac excitation. The resonance observed in the present case could be associated to the relaxing species at the grain–grain boundary interfaces.

To understand the features of interfacial polarization and resonance peaks observed in the tan δ vs. log ω behavior, the impedance spectra for the composites with

$y=0.5$ are determined, here Fig. 8a and b show the observed and simulated impedance spectra for 0.5MSBN composites sintered at 1160 and 1225 °C respectively. At present 0.5MSBN composite is selected for analysis, as this composition has shown maximum contribution of the interfacial polarization. Based on earlier work on thin film heterostructures, it is observed that impedance of ferrite ferroelectric composites could be expressed using an equivalent circuit as shown in Fig. 9 [34]. Here R_1C_1 and R_2C_2 correspond to the dielectric properties of the ferroelectric system, while the C_i represents contribution due to interfacial polarization. Making use of the curve fitting technique, as discussed earlier, the values of R_1, C_1, ω_{01}, R_2, C_2, ω_{02} and C_i are calculated. Here Table 4 shows variation of the equivalent circuit parameters for 0.5MSBN sintered at 1160 and 1225 °C. The Table 4 also shows the ratio of ω_{01}/ω_{02}. From Fig. 8a and b it is observed that the observed and simulated behavior match with each other over entire range of frequencies. Nevertheless the mismatch

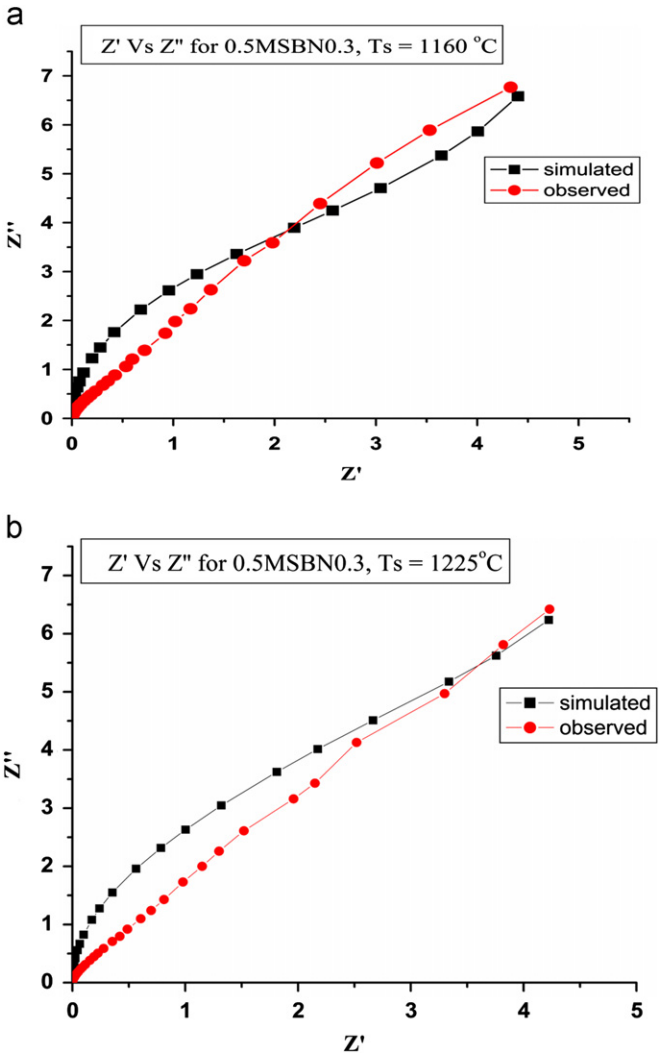

Fig. 8. (a) Variation of Z' vs. Z'' for 0.5MSBN0.3 composites sintered at 1160 °C and (b) Variation of Z′ vs. Z″ for 0.5MSBN0.3 composites sintered at 1225 °C.

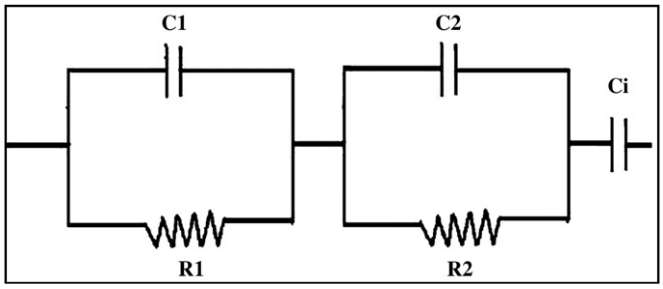

Fig. 9. Equivalent circuit model for magnetodielectric composites.

Table 4
Shows the variation of R_1, C_1, ω_{01}, R_2, C_2, ω_{02}, C_i and ω_{01}/ω_{02} for 0.5MSBN0.3 sintered at 1160 and 1225 °C.

Sample Name	R_1	C_1	ω_{01}	R_2	C_2	ω_{02}	C_i	ω_{01}/ω_{02}
0.5MSBN,1160	2.95	1994.018	170	2.65	751.7101	502	1750	2.95
0.5MSBN,1225	4.4	1208.897	188	1.2	877.3315	942	1990	5.01

error of less than 5% could be due to additional leakage capacitance present at grain surfaces. From Table 4 it is seen that the grain and grain boundary semicircles are fairly unresolved as ω_{01}/ω_{02} is less than 10 [35]. Thus it could be seen that dielectric properties of grain boundary did not differ drastically from the bulk of grain. The difference in grain and grain boundary properties could be attributed to the micro-chemical inhomogeneity. SBN being a relaxor material is known to possess frequency dependent transition temperature (T_c) this feature of relaxor material is predicted to be because of chemical inhomogeneity present in the material [16–18]. The inhomogeneity could be predominant at the grain surface and therefore the dielectric properties of grain and grain boundary may differ from each other. However from Table 4 it is observed that the total resistance R_1+R_2 does not change with the sintering temperature. Therefore the loss tangent is almost same for both the composites as seen in Fig. 10. Further as sintering temperature increases ω_{o1}/ω_{o2} increases from 2.95 to 5.01. This feature suggests that as sintering temperature increases the difference in grain and grain boundary properties increases. This feature may suggest that the inhomogeneity increases with sintering temperature. Further the interfacial capacitance also increases with increase in sintering temperature. This feature may occur because of increase grain growth at higher sintering temperature, which leads to increase in the voids between grains. The magnitude of interfacial capacitance is in nanofarad scale and therefore the contribution of interfacial polarization is substantial even for higher frequencies up to 100 kHz. This observation is sufficient to explain dispersion in ε' occurring up to very high frequencies that is less than 100 kHz. Further the same observation suggests that if the electrode contribution to the dielectric constant if exists, will be insignificant.

Fig. 11 shows variation of P–E hysteresis for parent SBN and composites 0.3MSBN0.3, 0.4MSBN0.3, 0.3MSBN0.1 and 0.4MSBN0.1 for $T_s=1160$ °C. Further Table 5 shows

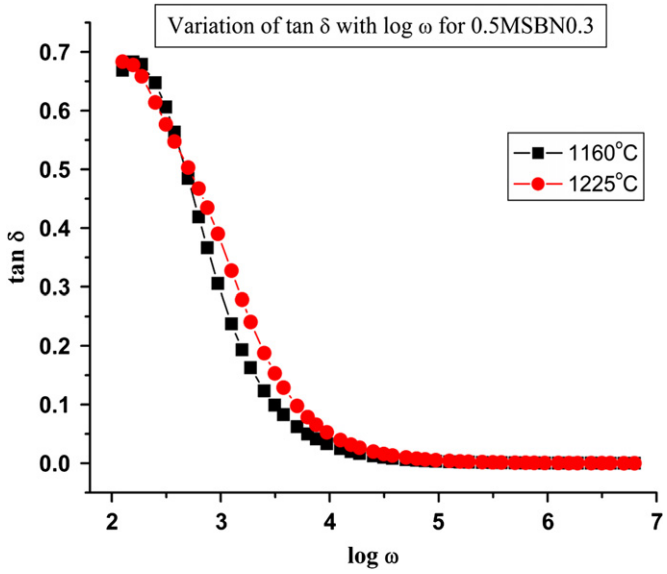

Fig. 10. Variation of tan δ vs. log ω for 0.5MSBN0.3 composites.

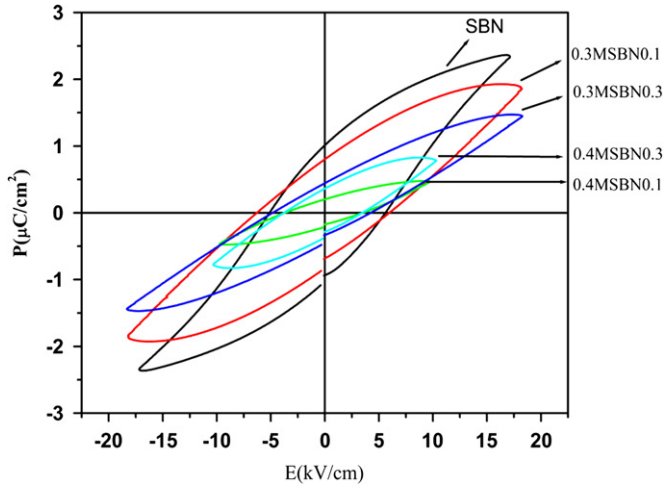

Fig. 11. Variation of *P–E* hysteresis for parent SBN and MSBN composites.

variation of P_{max} and P_r for the compositions specified above. The hysteresis loops of all the compositions correspond to the loops for polycrystalline ferroelectric compositions. From Table 5 it could be seen that for *y*MSBN0.1 as well as *y*MSBN0.3 the P_{max} decreases as *y* increases. The P_{max} increases with decreasing *y* could be correlated with the content of SBN phase. From Eqs. (1 and 2) it could be seen that the content of SBN phase increases with decrease in *y* thus the present observations.

Further it is interesting to note that the present composites also exhibits magneto hysteresis loops. The Table 6 shows the variation of saturation magnetization (M_s), remnant magnetization (M_r) and coercive field (H_c) as a function of *y* for *y*MSBN0.1 and *y*MSBN0.3 composites sintered at 1160 °C. It is observed M_s, M_r and H_c increases with increase in *y*. The present observations could be correlated with increasing content of CMFO0.1 or CMFO0.3 in the composites as *y* increases, Eqs. (1 and 2).

Table 5
Shows the variation of maximum polarization (P_{max}) and remnant polarization (P_r) for composites.

y	yMBSN*x*	P_{max} (μC/cm²)	P_r (μC/cm²)
0.0		2.36	1
0.3	$x=0.1$	1.88	0.82
0.4		0.44	0.20
0.3		1.46	0.46
0.4	$x=0.3$	0.80	0.4

Table 6
Shows the variation of saturation magnetization (M_s), remnant magnetization (M_r) and coercive field (H_c) composites.

y	*y*MBSN*x*	M_s	M_r	H_c (Oe)
0.3		44.27	10.29	180
0.4	$x=0.1$	70	19.11	240
0.5		94.27	25.48	240
0.3		24.32	6.9	90
0.4	$x=0.3$	63.7	14.15	210
0.5		100.76	19.11	210

3.2. Magnetoelectric effect

Linear and quadratic magnetoelectric coefficients α and β are determined using the following relation,

$$\alpha = (dv/dh)*1/t$$

and

$$\beta = (dv/dH)*1/2h$$

where v is the rms value of voltage developed across the sample in response to an ac magnetic field h. Further H is the applied dc magnetic field and t is the sample thickness. The details of measurement techniques are already discussed elsewhere [22]. In the present case both α as well as β are measured using a custom designed set-up as referred above.

Fig. 12 shows variation of α as a function of *y*, for the MSBN0.3 and MSBN0.1 composites, while Tables 7 and 8 show variation of α and β with *y*. In case of MSBN0.3 *y* is varied from 0.1 to 0.6, while for MSBN0.1 three selected values of *y* viz. 0.3, 0.4, 0.5 are selected. It is known that in case of composites, compositional variation of ME properties are determined by the relation $y*(1-y)$ which becomes maximum for $y=0.5$ [36]. Therefore in case of MSBN0.1, *y* is selected to be 0.3, 0.4, and 0.5. Further as per as the comparison between CMFO0.1 and CMFO0.3 is concerned, the CMFO0.1 possess lower value of ρ and large value of λ. Lower value of ρ may restrict maximum polling field that could be excited across the sample. Therefore the values of *y* are kept restricted. Further in both the cases the polling field applied was always greater than 15 kV/cm and

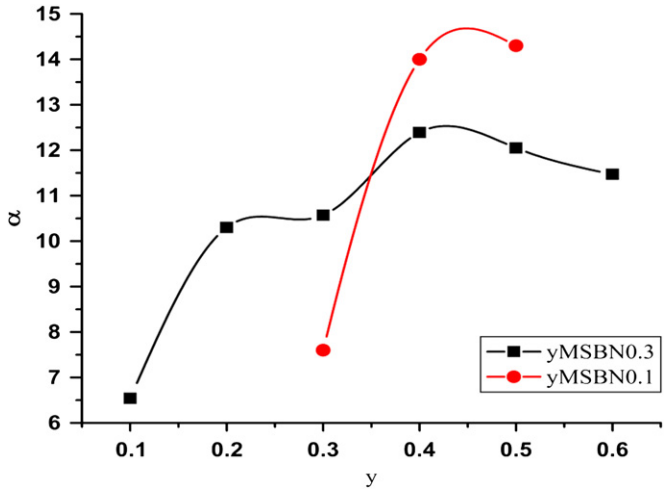

Fig. 12. Variation of α as a function of y, for the MSBN0.3 and MSBN0.1 composites.

Table 7
Variation of linear and quadratic magnetoelectric coefficient α and β with y for yMSBN0.3 composites.

y	α (1160 °C) (mv/Oe/cm)	α (1225 °C) (mv/Oe/cm)	$\beta*10^{-4}$ (1160 °C) (mv/Oe^2/cm)	$\beta*10^{-4}$ (1225 °C) (mv/Oe^2/cm)
0.2	10.3	7.5	2.72	0.7
0.3	10.569	8.33	2.39	1.0
0.4	12.39	14.42	3.01	2.0
0.5	12.05	8.43	2.40	0.4
0.6	11.47	9.57	0.670	0.09

Table 8
Variation of linear and quadratic magnetoelectric coefficient α and β with y for the composites yMBSN0.1 sintered at 1160 and 1225 °C.

y	α (1160 °C) (mv/Oe/cm)	α (1225 °C) (mv/Oe/cm)	$\beta*10^{-4}$ (1160 °C) (mv/Oe^2/cm)	$\beta*10^{-4}$ (1225 °C) (mv/Oe^2/cm)
0.3	7.6	12.2	20	5
0.4	14.0	10.5	8	10
0.5	14.3	6.6	5	20

the samples are polled at maximum field for 6 h in all the cases.

From the Fig. 12 and Tables 7 and 8 it is seen that the α becomes maximum for $y=0.4$ in case of MSBN0.3, while the magnitude of α saturates for $y=0.4$ and 0.5 in case of MSBN0.1. In this case α for MSBN0.1 is always greater than MSBN0.3, which could be associated to the higher value of λ in case of MSBN0.1. From the basic theory of ME properties it is known that α is proportional to a qualitative relation $\lambda*k_m*d/\varepsilon$ where λ is coefficient of magnetostriction, k_m—electromechanical coupling coefficient, d—piezoelectric coupling coefficient and ε is the dielectric constant. Further the use of Bi_2O_3 as a sintering aid may improve the electromechanical coupling coefficient k_m. In the present case α is measured at 850 Hz, usually at these frequencies ε is fairly high and the observed value of α appeared slightly low. Nevertheless as compared to the literature the magnitude of α 14 mv/cm/Oe too is also a large enough magnitude [37,38].

The quadratic magnetoelectric coefficient β occurs mainly because of the field dependence of coefficient of magnetostriction λ. As discussed above from the basic theory of ME effect the β is also proportional to $y*(1-y)*(\lambda*k_m*d*d\lambda/dH)/\varepsilon$, where $d\lambda/dH$ is the rate of change of coefficient of magnetostriction with magnetic field. Now ε may vary with the varying composition and β may exhibit proportionality with λ and y. The variation of β is shown in Fig. 13. Further β for yMSBN0.1 is always greater than yMSBN0.3. This observation could be correlated with the higher value of λ for CMFO0.1 as compared to CMFO0.3. It is observed that for $x=0.1$ β is maximum for $y=0.3$ and for $x=0.3$, β is fairly independent of y. Further it is known that the magnetocapacitance may show proportionality with β. This feature is discussed in further magnetodielectric properties.

3.3. Magnetodielectric effect

Figs. 14 and 15 show the variation of tan δ as a function of frequency and applied magnetic field for 0.4MSBN0.3 and 0.4MSBN0.1 sintered at 1225 °C respectively. Here tan δ passes through a maximum for a frequency just above 500 kHz which is expected to be the EMR resonance frequency for the radial mode of oscillations. It is also observed that the EMR frequency is independent of variations of y, x and T_s. This is expected because all the samples investigated possess diameter at 1.2 cm.

Interesting observations are on the variations of dielectric constant (ε) as a function of applied field that is the MD behavior. Here Figs. 16 and 17 show the variation of ε as a function of applied frequency (f) and applied magnetic field (H_{dc}) for 0.4MSBN0.3 and 0.4MSBN0.1 sintered at 1225 °C respectively. In the present case the MC is

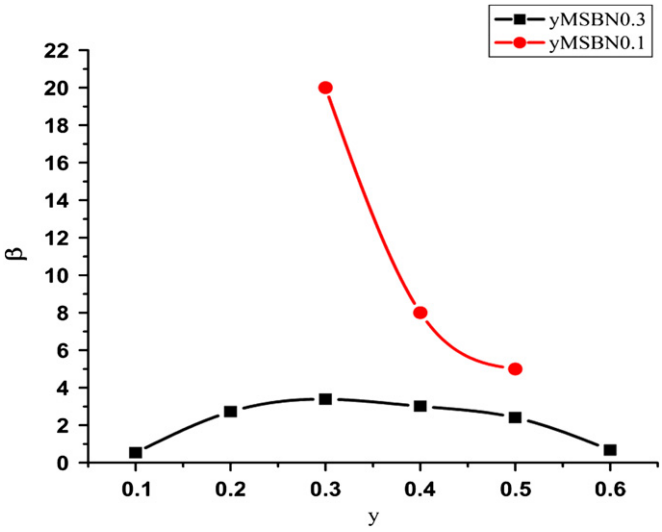

Fig. 13. Variation of β as a function of y, for the MSBN0.3 and MSBN0.1 composites.

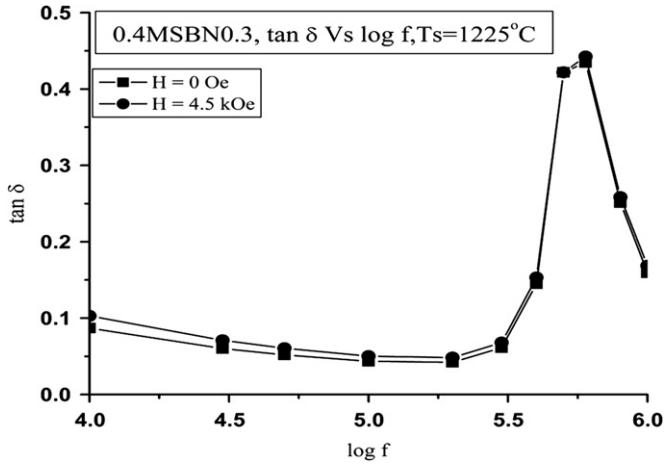

Fig. 14. Variation of $\tan\delta$ as a function of frequency and applied magnetic field for 0.4MSBN0.3 T_s=1225 °C.

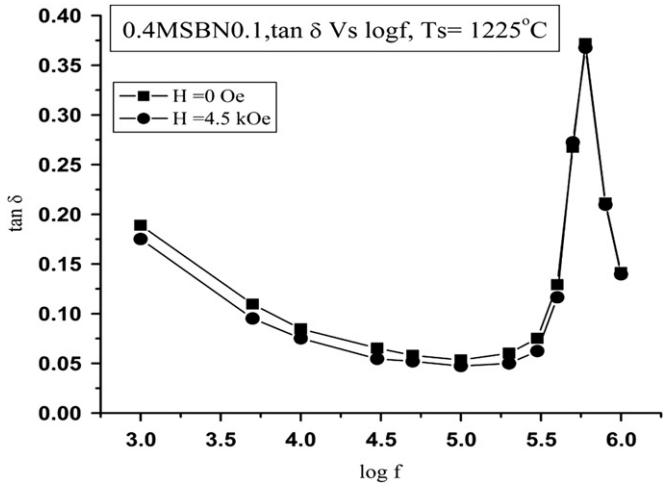

Fig. 15. Variation of $\tan\delta$ as a function of frequency and applied magnetic field for 0.4MSBN0.1 T_s=1225 °C.

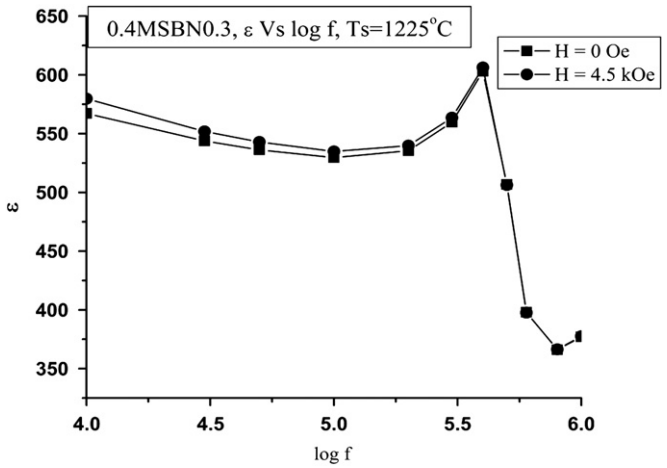

Fig. 16. Variation of ε as a function of frequency and applied magnetic field for 0.4MSBN0.3 T_s=1225 °C.

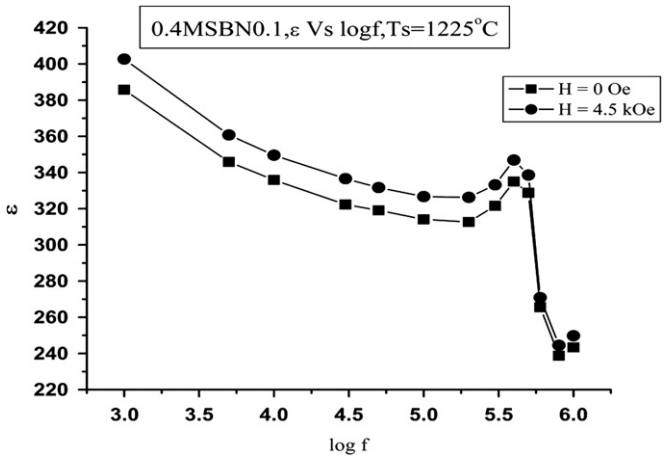

Fig. 17. Variation of ε as a function of frequency and applied magnetic field for 0.4MSBN0.1 T_s=1225 °C.

determined in the two separate configurations of applied magnetic field and applied ac electric field (E_{ac}). In case one H_{dc} as well as E_{ac} are along the axis of disc while in case two H_{dc} is along the radius of disc and E_{ac} is along the direction of disc axis. Figs. 16 and 17 represent the observations of case one. Here the variation of ε for other composition and sintering temperature T_s are similar in nature as shown in Figs. 16 and 17. Table 9 shows the variation of MC as a function of T_s both for case one and case two for yMSBN0.1 and frequencies f=10 and 500 kHz respectively. It is observed that the MC in case one is large as compared to case two, therefore only the variation of case one is recorded for yMSBN0.3 composites and shown in Table 10.

As a part of discussion on MC, it is interesting to note the following behavior. As discussed earlier, the MC occurs due to variation of dielectric constant because of the applied stress occurring due to the piezomagnetic effect in the ferrite phase [7]. Further the MC should be

Table 9
Magneto capacitance (MC) for yMBSN0.1.

Y	MC(1160°C) %				MC(1225°C) %			
	Parallel		*Perpendicular*		*Parallel*		*Perpendicular*	
	10 kHz	500 kHz	10 kHz	500 kHz	10 kHz	500 kHz	10 kHz	500 kHz
0.3	2.2	1.2	−0.9	−0.3	0.5	0.15	−0.76	−0.3
0.4	0.17	0	−0.13	−0.1	4.2	3.1	−0.8	−0.5
0.5	0.45	0.14	−0.35	−0.01	2.2	1.2	−0.8	−0.6

proportional to $\lambda * k_m * (d\varepsilon/ds)$, where λ is magnetostrictive coefficient, k_m magnetomechanical coupling coefficient and $d\varepsilon/ds$ is rate of change of dielectric constant as a function of applied stress. For λ being positive, the stress will increase with increase in H_{dc}, while for λ negative stress would decrease with increase in H_{dc} and therefore ε decreases with H_{dc} for λ being positive and ε increases with H_{dc} for λ being negative.

Table 10
Magneto capacitance (MC) for yMBSN0.3.

y	MC(1160 °C) (%) parallel		MC(1225 °C) (%) parallel	
	10 kHz	500 kHz	10 kHz	500 kHz
0.3	0.86	0.4	0.16	0
0.4	1.2	0.2	0.9	0.08
0.5	0.6	0.2	0.93	0.51

As discussed by Gridnev et.al. the increase in stress will cause increase in P_{max} and therefore the ε decreases for increase in stress and vice versa [7]. As ε decreases for increase in stress the MC will be negative for positive λ and positive for negative λ. Further it is already reported and discussed that the $\lambda_{\parallel}$ (parallel) is negative for CMFO composition while $\lambda_{\perp}$ (perpendicular) is positive [11,12]. Also it is observed that $\lambda_{\parallel}$ is almost double that of $\lambda_{\perp}$. As a conclusion of above discussion it is expected that in case of case one, where H_{dc} is parallel with E_{ac}, $\lambda_{\parallel}$ will play its role in determination of MC, that is as H_{dc} increases the stress reduces and ε increases, and MC is positive. Inverse will be the situation for case two and MC is negative. It is also expected that $MC_{\parallel}$ (parallel) should be almost double of $MC_{\perp}$ (perpendicular) as a outcome of the comparative magnitude of $\lambda_{\parallel}$ and $\lambda_{\perp}$.

The present observations are in confirmation with the qualitative logic as discussed in the above paragraph. Here MC is positive for case one while it is negative for case two. Also magnitude of $MC_{\parallel}$ is sufficiently large as compared to $MC_{\perp}$. As a part of variation of MC with y it is seen that α is maximum for $y=0.4$ probably due to $y*(1-y)$ relationship for the ME compositions. Further it is also observed that the MC increases for increasing β. From Table 8 it is seen that for yMSBN0.1, β is high for $T_s=1225$ °C as compared to $T_s=1160$ °C. Therefore the MC should become maximum for $T_s=1225$ °C and $y=0.4$. The present observations are in confirmation with the logic mentioned above. The magnitude of MC is significant in the present case that is of 4.2%. Further it is observed that unlike the MC due to the variation of interfacial polarization, the strain induced MC in present case is fairly large even up to the EMR frequencies at nearly 500 kHz.

3.4. Conclusions

The dielectric properties of composites show the presence of ferroelectric behavior of SBN and also presence of interfacial polarization. The ferroelectric contribution decreases with y, while the contribution of interfacial polarization is proportional to $y(1-y)$ relationship. The interfacial polarization is predominant at lower frequencies and at higher temperatures as expected on the basis of the Maxwell–Wagner Model. α is observed to follow the $y(1-y)$ proportionality and also α is observed inversely proportional to dielectric constant (ε). Magnetocapacitance (MC) occurs due to variation of dielectric constant (ε) because of the applied stress occurring due to the piezomagnetic effect in the ferrite phase. As ε decreases for increase in stress the MC will be negative for positive values of λ and MC is positive for negative values of λ. λ for CMFO is observed to be negative when the applied magnetic field is in the direction of measurement of strain, while λ is positive for the applied magnetic field perpendicular to the direction of measurement of strain. The present observations show that the MC is positive for applied magnetic field parallel to the strain and MC is negative when applied magnetic field is perpendicular to the direction of strain. Further it is observed that the strain induced MC in present case is fairly large even up to the EMR frequencies at nearly equal to 500 kHz. Thus present observations are in confirmation with the theoretical predictions based on Gridnev's theoretical model. The M_c is observed to be proportional to the quadratic magnetoelectric coefficient β because of the coefficient of magnetostriction (λ) being proportional to magnetic field (H).

References

[1] M. Liu, O. Obi, J. Lou, S. Stoute, Z. Cai, K. Ziemer, N.X. Sun, Strong magnetoelectric coupling in ferrite/ferroelectric multiferroic heterostructures derived by low temperature spin-spray deposition, Journal of Physics D: Applied Physics 42 (2009) 045007 (5pp).

[2] A. Yu., V.L. Ostashchenko, Preobrazhenskii, P. Pernod, Magnetoelectric effect in an asymmetric layered magnet-piezoelectric structure, Physics of the Solid State 50 (2008) 463–468.

[3] J. Ma, Z. Shi, Gong, C.W. Nan, Magnetic-field induced electric response of simple magnetoelectric composite rods, Journal of Physics D: Applied Physics 41 (2008) 155001 (6pp).

[4] X.W. Dong, Y.J. Wu, J.G. Wan, T. Wei, Z.H. Zhang, S. Chen, H. Yu, J.M. Liu, Phase shift of electric-field-induced magnetization in magnetoelectric laminate composite, Journal of Physics D: Applied Physics 41 (2008) 035003 (4pp).

[5] X.M. Chen, Y.H. Tang, Dielectric and magnetoelectric characterization of $CoFe_2O_4/Sr_{0.5}Ba_{0.5}Nb_2O_6$ copmosites, Journal of Applied Physics 96 (2004) 11.

[6] Y.J. Li, X.M. Chen, Y.Q. Lin, Y.H. Tang, ME effect of $Ni_{0.8}Zn_{0.2}Fe_2O_4/Sr_{0.5}Ba_{0.5}Nb_2O_6$ composites, Journal of European Ceramic Society 26 (2006) 2839.

[7] S.A. Gridnev, A.V. Kalgin, V.A. Chernykh, Magnetodielectric effect in two-layer magnetoelectric PZT-MZF composite, Integrated Ferroelectrics 109 (2009) 70–75.

[8] C.G. Zhong, Q. Jiang, Theory of the magnetoelectric effect in multiferroic epitaxial $Pb(Zr_{0.3}Ti_{0.7})O_3/La_{1.2}Sr_{1.8}Mn_2O_7$ heterostructures, Journal of Physics D: Applied Physics 41 (2008) 115002 (6pp).

[9] J.V.D. Boomgaard, R.A.J. Born., A sintered magnetoelectric composite material $BaTiO_3$-Ni(Co,Mn)Fe_2O_4, Journal of Materials Science 13 (1978) 1538.

[10] R.P. Mahajan, K.K. Patankar, M.B. Kothale, S.C. Chaudhari, V.L. Mathe, S.A. Patil, ME effect in cobalt ferrite–barium titanate composites and their electric properties, Pramana: Journal of Physics 58 (2002) 1115.

[11] S.D. Bhame, P.A. Joy, Enhanced magnetostrictive properties of Mn substituted cobalt ferrite $Co_{1.2}Fe_{1.8}O_4$, Journal of Applied Physics 99 (2006) 073901.

[12] S.D. Bhame, P.A. Joy, Magnetic and magnetostrictive properties of manganese substituted cobalt ferrite, Journal of Applied Physics 40 (2007) 3263.

[13] O. Caltun, C. Chiriac, N. Lupu, I. Dumitru, B.P. Rao, High magnetostrictive doped cobalt ferrite, Journal of Optoelectronics and Advanced Materials 9 (2007) 1158.

[14] J.A. Paulsen, A.P. Ring, C.C.H. Lo, Manganese-substituted cobalt ferrite magnetostrictive materials for magnetic stress sensor applications, Journal of Applied Physics 97 (2005) 044502.
[15] Xu Gang, Weng Wenjian, Yao Jianxi, Du Piyi, Han Gaorong, Low temperature synthesis of lead zirconate titanate powder by hydroxide co-precipitation, Microelectronic Engineering 66 (2003) 568.
[16] M.P. Pathak, P.K. Patro, A.R. Kulkarni, Dielectric properties of strontium barium niobate synthesized by Pechini method, in: Proceedings of the National Seminar on Ferroelectrics and Dielectrics XIII, 2004, 9 206.
[17] A.R. Kulkarni, P.K. Patro, C.S..Harendranath, Explaining the effect of homogeneity on microstructure, dielectric and ferroelectric properties of strontium barium niobate, in: Proceedings of the National Seminar on Advances in Electroceramics 2006, 2006 55.
[18] P.K. Patro, R.D. Deshmukh, A.R. Kulkarni, C.S. Harendranath, Journal of Electroceramics 13 (2004) 479–485.
[19] A. Speghini, M. Bettinelli, U. Caldiño, M.O. Ramírez, D. Jaque, L.E. Bausá, J. García Solé, Journal of Physics D: Applied Physics 39 (2006) 4930–4934.
[20] C. David, T. Granzow, A. Tunyagi, M. Wöhlecke, Th. Woike, K. Betzler, M. Ulex, M. Imlau, R. Pankrath, Physica Status Solidi A 201 (8) (2004) R49–R52.
[21] S.S. Veer, D.J. Salunkhe, S.V. Kulkarni, P.B. Joshi, Effect of sintering aid on physical and magnetoelectric properties of $La_{0.7}Sr_{0.3}MnO_3$-$BaTiO_3$, Indian Journal of Engineering and Material Science 15 (2008) 121.
[22] D.J. Salunkhe, S.S. Veer, S.V. Kulkarni, S.B. Kulkarni, P.B. Joshi, Experimental setup for the measurement of magneto-electric susceptibilities for different composites, Journal of Instrumentation Society of India 38 (4) (2008) 294–298.
[23] S.R. Jigajeni, S.V. Kulkarni, Y.D. Kolekar, S.B. Kulkarni, P.B. Joshi, $Co_{0.7}Mg_{0.3}Fe_{2-x}Mn_xO_4$–$Sr_{0.5}Ba_{0.5}Nb_2O_6$ magnetoelectric composites, Journal of Alloys and Compounds 492 (2010) 402.
[24] J. Ross Macdonald, Annals of Biomedical Engineering 20 (1992) 289–305.
[25] S. Sherrit, N. Gauthier, H.D. Wiederick, B.K. Mukherjee, S.E. Prasad, IEEE 7th International Symposium on Applications of Ferroelectrics, 1990, 346–349. 0-7803-0190-0/91$0 1.00.
[26] Chi-Jen Chen, Jenn-Ming Wu, Journal of Materials Research 5 (1990) 1530–1537.
[27] Antonio Ming Li, Feteira, Derek C. Sinclair, Journal of Applied Physics 105 (2009) 114109.
[28] R.P. Tandon, Impedance spectroscopy of lanthanum modi-ed $Pb(Zr,Ti)O_3$, Ceramics Journal of the Korean Physical Society 32 (February) (1998) S327–S329.
[29] B. Barbier, C. Combettes, S. Guillemet-Fritsch, T. Chartier, F. Rossignol, A. Rumeau, T. Lebey, E. Dutarde, Journal of the European Ceramic Society 29 (4) (2009) 731–735.
[30] Sergei V. Kalinin, Matthew R. Suchomel, Peter K. Davies, Dawn A. Bonnell, Journal of the American Ceramic Society 85 (12) (2002) 3011–3017.
[31] K.W. Wagner, Annals of Physics (Amsterdam, Netherlands) 40 (1993) 818.
[32] C.G. Koops, Physical Review 6 (1997) 108.
[33] A. Ianculescu, D. Berger, L. Mitoşeriu, L.P. Curecheriu, N. Drăgan, D. Crişan, E. Vasile, Ferroelectrics 369 (1) (2008) 22–34.
[34] A.N. Tarale, Y.D. Kolekar, V.L. Mathe, S.B. Kulkarni, V.R. Reddy, Pradeep Joshi, Electronic Materials Letters 8 (4) (2012) 381–385.
[35] L. Pandey, Om Parkash, R.K. Katare, D. Kumar, Bulletin of Materials Science 18 (1995) 563.
[36] G. Shrinivasan, E.T. Rasmussen, J. Gallegal, R. Shrinivasan, Magnetoelectric bilayer and multilayer structures of magnetostrictive and piezoelectric oxides, Physical Review B 64 (14408) (2001).
[37] Yun Zhoua, Jincang Zhanga, Li Lia, Yuling Sua, Jinrong Chengb, Shixun Cao, Journal of Alloys and Compounds 484 (2009) 535–539.
[38] C.M. Kanamadi, J.S. Kim, H.K. Yang, B.K. Moon, B.C. Choi, J.H. Jeong., Journal of Alloys and Compounds 481 (2009) 781–785.